Metallic ferroelectricity induced by anisotropic unscreened Coulomb interaction in $LiOsO_3$

H. M. Liu,[1] Y. P. Du,[1] Y. L. Xie,[1] J.-M. Liu,[1] Chun-Gang Duan,[2] and Xiangang Wan[1,*]

[1]*National Laboratory of Solid State Microstructures, School of Physics, Collaborative Innovation Center of Advanced Microstructures, Nanjing University, Nanjing 210093, China*

[2]*Key Laboratory of Polar Materials and Devices, Ministry of Education, East China Normal University, Shanghai 200062, China*

(Received 27 October 2014; revised manuscript received 27 January 2015; published 20 February 2015)

As the first experimentally confirmed ferroelectric metal, $LiOsO_3$ has received extensive research attention recently. Using density-functional calculations, we perform a systematic study on the origin of the metallic ferroelectricity in $LiOsO_3$. We confirm that the ferroelectric transition in this compound is order-disorder-like. By doing electron screening analysis, we unambiguously demonstrate that the long-range ferroelectric order in $LiOsO_3$ results from the incomplete screening of the dipole-dipole interaction along the nearest-neighboring Li-Li chain direction. We conclude that highly anisotropic screening and local dipole-dipole interactions are the two most important keys to form $LiOsO_3$-type metallic ferroelectricity.

DOI: 10.1103/PhysRevB.91.064104 PACS number(s): 77.80.B−, 61.50.Ah, 71.20.−b, 72.80.Ga

I. INTRODUCTION

Ferroelectric (FE) instability can be explained by a delicate balance between short-range elastic restoring forces supporting the undistorted paraelectric (PE) structure and long-range Coulomb interactions favoring the FE phase [1]. Itinerant electrons can screen the electric fields and inhibit the electrostatic forces; metallic systems are thus not expected to exhibit ferroelectric-like structural distortion. Despite the incompatibility, using a phenomenological theory, Anderson and Blount proposed in 1965 that metals can break inversion symmetry [2]. They found that the FE metal is possible through a continuous structural transition accompanied by the appearance of a polar axis and the disappearance of an inversion center [2]. Very recently, Puggioni and Rondinelli propose a microscopic mechanism about how to eliminate the incompatibility between metallicity and acentricity [3]. In 2004, $Cd_2Re_2O_7$ had been proposed as a rare example of ferroelectric metals [4]; however, it was found that although this compound exhibits a second-order phase transition to a structure that lacks inversion symmetry a unique polar axis could not be identified [5], which does not fit the criteria about the FE metal.

In 2013, the first convincing success was achieved experimentally in $LiOsO_3$ [6]. $LiOsO_3$ remains metallic behavior while it undergoes a second-order phase transition from the high-temperature centrosymmetric $R\bar{3}c$ to a FE-like $R3c$ structure at $T_s = 140$K [6]. Neutron and x-ray-diffraction studies showed that the structural phase transition involves the displacements of Li ions accompanying also a slight shift of O ions [6]. The electronic structure and lattice instability were studied by several groups [7–9]. It was found that the local polar distortion in $LiOsO_3$ is solely due to the instability of the *A*-site Li ion [7–9]. The importance of the Coulomb interaction among 5*d* electrons and the hybridization between oxygen *p* orbitals and Os empty e_g orbitals has also been emphasized by Giovannetti and Capone [9]. Despite these efforts devoted to understanding the origin of the FE-like structural transition in this metallic system, there are still two fundamental issues that have not been clearly clarified. The first is the origin of the ferroelectric instability: is it displacive or order-disorder? Second, as the FE-like phase transition of $LiOsO_3$ occurs at a relatively high temperature (140 K), how can these local dipoles line up to form long-range order, as if there are no conduction electrons to screen the dipole interactions?

In this paper, based on the density-functional theory (DFT) calculations, we reveal the microscopic mechanism for the FE-like structural transition in $LiOsO_3$. Our study shows that, different from other 5*d* transition-metal oxides [10–12,14], for $LiOsO_3$, the effect of spin-orbital coupling (SOC) is small and the electronic correlation is weak. Our comprehensive potential surface calculations suggest that the structural transition is order-disorder-like. The most striking finding is that the electric screening in $LiOsO_3$ is highly anisotropic despite its metallic nature. Consequently, the dipole-dipole interactions are unscreened along certain directions, which results in the long-range FE order at considerably high temperature. This is in sharp contrast to the case in the displacive type FE compounds, where the FE structural transition is usually driven by hybridization or a lone pair [17], and consequently the change of the electric dipole (namely, the atomic motion) will modify the valence band significantly. If such displacive type FE compounds become metallic, the interactions between their electric dipoles will be strongly screened out, and the metallic FE phase is highly unlikely to occur.

Before the formal presentation of the calculated results, we would like to first discuss our strategy to study the electric screening effect. As is well known, the major difference between the insulator and metal is that there are free nonlocalized electrons in metals, whereas in insulators there are only bound electrons. Consequently, electrostatic forces will be strongly screened by the itinerant electron in the metallic system. The screening effect actually can be described as the electron charge difference induced by a perturbation such as the change of the dipole or external electric field [18]. However, seldom efforts have been carried out to study the screening effect in the bulk metal, as people generally believe there is no macroscopic electric field inside metals. In the current study, we try to study the electric response to a local dipole in the bulk metal. This is done by analyzing the charge difference before and after the local dipole is introduced. Such a strategy provides an explicit

*Corresponding author: xgwan@nju.edu.cn

picture on the exact behavior of the screening effect in metallic systems.

II. METHOD

Our first-principles calculation is performed using the VASP (Vienna *ab initio* simulation package) code [19,20]. The results presented in the following are obtained by using the generalized gradient approximation (GGA) Perdew-Becke-Erzenhof (PBE) function [21], a $20\times20\times20$ mesh for the Brillouin-zone sampling and 500 eV for cutoff of the plane-wave basis set. The effect of the exchange-correlation function pseudopotential cutoff value has been carefully checked, and some of the results are shown in the Appendix.

III. RESULTS AND DISCUSSIONS

There are ten atoms in the primitive unit cell of $LiOsO_3$. The atomic arrangements are sketched in Fig. 1. In the $R\bar{3}c$ PE structure, the Os atoms are at the centers of the oxygen octahedrons, while Li atoms are centered between two adjacent Os atoms along the polar axis on average. Using the experimental lattice parameters, we optimize all independent internal atomic coordinates of the FE structure until the Hellman-Feynman forces on every atom are converged to less than 1 meV/Å; the optimized internal atomic coordinates are listed in Table I, and the experimental PE and FE structures have also been presented in Table I for comparison. The calculated results coincide with previous experimental and calculated results [6–9], and the FE structural phase transition mainly involves the displacements of Li atoms: Li atoms shift along the polar axis about $d \sim 0.47$ Å from the mean positions of the PE phase [see gray arrow d in Fig. 1(a)] and O atoms slightly displace about 0.056 Å [6,7,9].

Based on calculated lattice structure, we first perform standard GGA calculation to see the basic features of the electronic structure of $LiOsO_3$. We show the total and partial density of states (DOS) in Fig. 2. Our results are consistent with previous work [6,7]. The energy range -9.0 to -2.4 eV is dominated by the O-2p orbital with an additional contribution from the Os-5d state, indicating hybridization between them. Notice that the phase transition involves a slight shift of O ions; the hybridization between Os-5d and O-2p states may have a finite contribution to the ferroelectric-like transition as discussed in Ref. [9]. As shown in Fig. 2(c), Li is highly ionic and its bands are far from the Fermi level. The Os atom is octahedrally coordinated by six O atoms, making the Os 5d band split into the t_{2g} and e_g states, and the t_{2g} bands are located from -2.2 to 1.2 eV, as shown in Fig. 2(c). Due to the extended nature of 5d states, the crystal splitting between t_{2g} and e_g states is large, and the e_g states are located about

TABLE I. Atomic positions (in primitive rhombohedral coordinates) in PE and FE phases. The experimental results are from Ref. [6].

	Atom	Position
PE	Li	(0.25, 0.25, 0.25)
	Os	(0,0,0)
	O	(0.8798, −0.3798, 0.25)
FE (Expt.)	Li	(0.2147, 0.2147, 0.2147)
	Os	(0,0,0)
	O	(0.8785, −0.3837, 0.2627)
FE (Calc.)	Li	(0.2149, 0.2149, 0.2149)
	Os	(0,0,0)
	O	(0.8855, −0.3842, 0.2557)

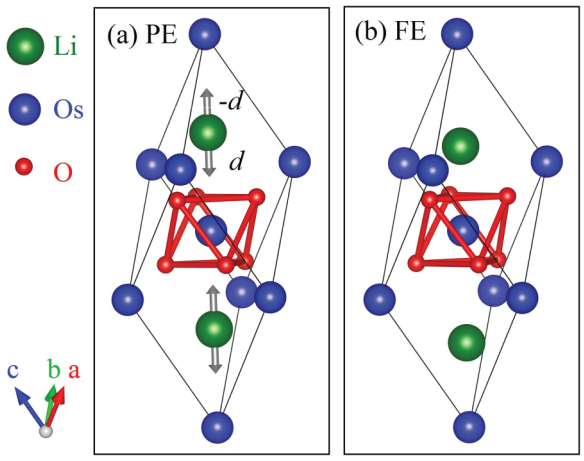

FIG. 1. (Color online) Primitive unit cell of (a) PE and (b) FE phases of $LiOsO_3$. The green, blue, and red balls are the Li, Os, and O ions, respectively. d and $-d$ correspond to the displacements of Li ions along the polar axis.

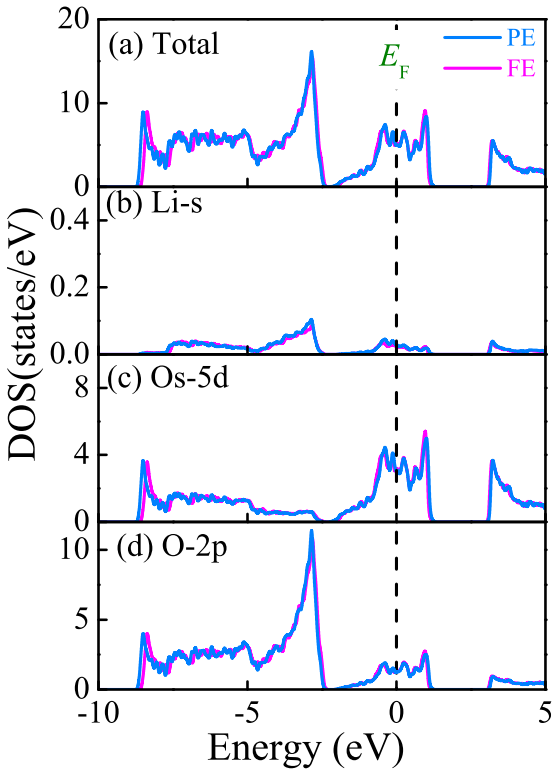

FIG. 2. (Color online) (a) The total DOS patterns of $LiOsO_3$ in PE (blue) and FE (pink) phases. The partial DOS of (b) Li-1s, (c) Os-5d, and (d) O-2p states in PE (blue) and FE (pink) phases, respectively. The Fermi energy is positioned as zero.

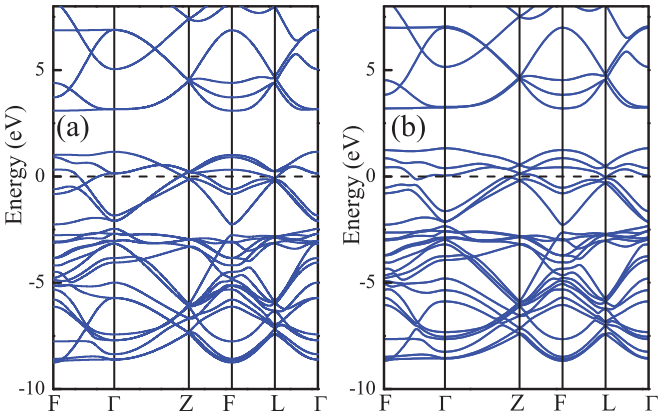

FIG. 3. (Color online) Band structure of $LiOsO_3$, shown along the high-symmetry directions. (a) GGA. (b) GGA + SO.

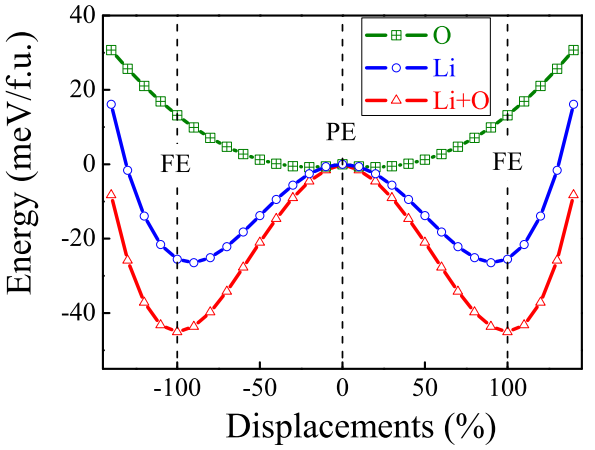

FIG. 4. (Color online) The olive, blue, and red curves represent the potential-energy changes with respect to O displacements only, Li displacements only, and the coupled displacements of the Li and O ions. The total energy and displacements of PE states are set as zero. The displacements of corresponded FE states are set as 100%.

3.0 eV higher than the Fermi energy and disperse widely. As shown in the comparison of DOS of PE and FE, the electronic structures almost do not change during the phase transition, which is consistent with the previous theoretical work [7]. It is worth mentioning that this is quite different from prototype FE systems such as $BaTiO_3$, in which hybridization is necessary for the FE phase transitions [22–24]. Thus we think the hybridization is not the major driving force for the structural instability in $LiOsO_3$.

It is well known that the SOC of 5*d* electrons is very strong [25] and usually changes the 5*d* band dispersion significantly, as demonstrated in Sr_2IrO_4 [10], pyrochlore iridates, and spinel osmium [11,12]. In the case of $LiOsO_3$, as shown in Fig. 2, the O-2*p* orbitals are almost fully occupied, while the bands of Li are mainly empty; thus Os occurs in its 5+ valence state and there are basically three electrons in its t_{2g} band. Since the t_{2g} band is half filled, it is natural to expect the effect of SOC to be small despite the large strength of SOC [13,15,16]. This has been confirmed by the comparison of the band structures obtained in the presence and absence of SOC. The SOC slightly enhances the t_{2g} bandwidth as shown in Fig. 3. Besides this, the band-structure difference around the Fermi level is small.

Although the 5*d* orbitals are spatially extended, it has been found that the electronic correlations are important for 5*d* transition-metal oxides [10–14]. The values of electronic correlation U obtained in Sr_2IrO_4/Ba_2IrO_4 are between 1.43 and 2.35 eV [14]. Although the accurate value of U is not known for this system, we generally expect screening to be larger in three-dimensional systems than in two-dimensional systems like Sr_2IrO_4. Furthermore, the Os-Os bond length of $LiOsO_3$ is shorter than that of $NaOsO_3$; thus we expect that the U in $LiOsO_3$ is even smaller than in $NaOsO_3$, for which U is around 1 eV [13]. Here, we estimate the Sommerfeld coefficient based on the numerical DOS at the Fermi level. Our numerical result (6.1 mJ mol^{-1} K^{-2}) is just slightly less than that of the experimental one (γ = 7.7 mJ mol^{-1} K^{-2}) [6], which indicates that the electronic correlation is indeed weak in $LiOsO_3$.

One fundamental issue about this system is the mechanism for the ferroelectric instability: is it displacive or order-disorder? Using comprehensive total-energy calculations, we now try to solve this issue. Following the common procedure used in the study of FE structures, we first calculate the potential-energy profile along different displacive soft modes, i.e., the evolution paths from the PE structure to the FE structure. The results, as shown in Fig. 4, suggest that the energy difference between the PE and FE structures is

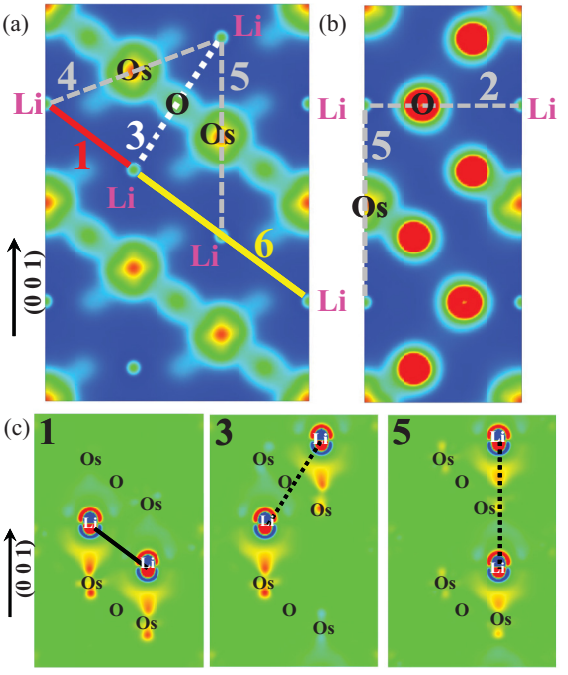

FIG. 5. (Color online) Partial electron densities contour maps for PE $LiOsO_3$ taken through (a) [1 -1 0] and (b) [2 -1 0] planes. Contour levels shown are between 0 (blue) and 0.3 e/Å^3 (red). (c) Charge density difference between FE and PE structures for Li pair 1, 3, and 5 through the [1 -1 0] plane. See text for details. Contour levels shown are between −0.004 (blue) and 0.004 e/Å^3 (red). The (0 0 1) direction here is the same as the (1 1 1) direction in Fig. 1.

majorally contributed by Li ion movements. The depths of double wells resulting from the motion of Li ions only and both of the Li and O ions are 27 and 44 meV, respectively, which is consistent with several previous works [7,9]. Note that we find that it is important to adopt the optimized structure to obtain the correct potential-energy surfaces. Adopting experimental coordinates will obtain unreasonable results, as the well depth caused by the sole Li ion movements is even larger than that of both the Li and O moments (see Fig. 6).

Nevertheless, we notice that the experimental transition temperature of $LiOsO_3$ is 140 K and much lower than the depths of double wells. This indicates that the transition in $LiOsO_3$ is most probably order-disorder-like [26]. This may also explain the experimentally observed incoherent charge transport above the transition temperature [6], which is possibly caused by the scattering induced by disorder of Li off-center displacement. For order-disorder transition, the Li atoms oscillate between the double wells, and the potential wells remain basically unchanged throughout the phase transition; thus we expect that there is no softening mode in the Raman spectra of $LiOsO_3$. Therefore, a Raman measurement is useful to clarify this issue.

As mentioned above, the Li ions in $LiOsO_3$ favor an off-center displacement and form local dipoles as shown in Fig. 1. Thus it is a puzzle why the local electric dipoles in different unit cells can interact with each other and form a long-range order at 140 K, noticing that the distance between them is far (even the nearest-neighbor dipole distance is larger than 3.5 Å) and the DOS at the Fermi level is rather large (Fig. 2). We find that the bands located below -10 eV are quite narrow and have negligible hybridization with other bands. The electrons at these bands are tightly bounded with the ion, and thus almost do not change with the motion of the Li ion; namely, these electrons almost have no contribution to the electric screening effect. On the other hand, the displacements of Li ions just slightly affect the Os-5d and O-2p electrons, as shown in Fig. 2. To have a straightforward view of the charge distribution, we sketched the electron densities of PE $LiOsO_3$ arising from states between -10 eV and the Fermi level in Figs. 5(a) and 5(b). There are two distinctive characters in these two figures. One is that the electronic density is relatively high between the Os and O ions, which again indicates the strong hybridization between Os-5p and O-2p states. The second is that there is almost no conduction charge at all in a relative large space around the Li ions; i.e., the Li ion is literally a *bare* ion. We will demonstrate later that the later character directly results in incomplete electric screening of dipole-dipole interactions and forms long-range dipole ordering.

Following the previously described procedure, we then demonstrate the screening effect by doing charge difference calculation. Since the FE-like transition basically involves displacements of Li ion, the change of local dipole can be approximated by the Li movement from the PE structure and the dipole interactions can be labeled as Li-Li pairs. In Fig. 5, we use, e.g., symbols 1, 2, and 3 to denote the Li-Li pairs with the first-, second-, and third-nearest distance between them. As is clear in Fig. 5(a), there is almost no conduction charge distribution between pair 1 (red solid line), and thus it is natural to expect the screening effect for the nearest dipole-dipole interaction to be small. This was confirmed by the calculation of the charge difference induced by the Li motions. We first construct a $3\times3\times1$ supercell containing 270 atoms in a hexagonal phase. The PE structure is taken as background. Then we move Li ions in pair 1 to their FE positions, and all other atoms are fixed. In this way we can see what happens when the two local dipoles are formed. The charge density change (namely, $\Delta\rho = \rho_{\mathrm{FE}} - \rho_{\mathrm{PE}}$) is then plotted in the left panel of Fig. 5(c), which clearly demonstrates the screening of these two dipoles. As can be seen from this plot, significant conduction electron responses only occur around Os ions, and they form local dipoles against the Li dipoles; this is exactly the screening effect which is expected in metallic systems. On the other hand, the charge distribution near O remains almost unchanged, indicating that the Os-5d and O-2p hybridizations are neither important for the electric dipole interaction nor affected by the Li dipoles. The most interesting thing is, as shown in the left panel of Fig. 5(c), that there is almost no modification of charge distribution in pair 1 at all. This clearly demonstrates that dipole interaction in pair 1 is only slightly screened. We then apply the same strategy to study other Li pairs. For pair 2 [Fig. 5(b)], as there is an O atom between two Li ions, we observe noticeable screening to prevent the direct dipole interaction. However, for pair 3, the dipole interaction is again not fully screened, as shown in the middle panel of Fig. 5(c). Detailed analysis indicates that this is because this Li pair is 0.65 Å away from the O ion plane. For other pairs, as there is either an O or Os atom between two Li ions, the electric screening effect is strong. The example of pair 5, which is also at the [1 −1 0] plane like pairs 1 and 3, is shown in the right panel of Fig. 5(c) for comparison.

Above, we have provided a qualitative picture about why locale dipole interactions are not fully screened in $LiOsO_3$. To give a more quantitative explanation, we try to estimate the interaction strength between the local electric dipole moments. Again using the above adopted supercell, we obtain coupling constant J_i ($i = 1$–6) between the ith Li pairs from the energy difference between the local FE and antiferroelectric (AFE) states (ith Li pairs are AFE ordered), i.e., $J_i = [E_{\mathrm{FE}} - E_{\mathrm{AFE}}]/2$. The Li-Li distances d_i of each pair and the obtained interaction parameter J_i are listed in Table II. Consistent with the above screening discussions, J_1 and J_3 are much larger than all other interactions, indicating that the dipole interactions are highly anisotropic. Despite d_6 being longer than d_2, d_4, and d_5, J_6 is considerably larger than J_2, J_4, and J_5, as shown in Table II, which also indicates the anisotropic screening effect in this metallic compound.

To show that these dipole interaction parameters obtained in the above procedure are reasonable, we perform Monte Carlo (MC) simulations using an effective Ising-like Hamiltonian: $H = \sum_i J_i D_m D_n$, where J_i is the coupling constant between dipole moments D_m and D_n. The obtained phase transition temperature is 210 K with only J_1 considered and 330 K with both J_1 and J_3 considered, which is reasonably higher than the experimental T_s (140 K), and the overestimation may come from the rigid dipole model used in our MC simulations. This, again, shows that our explanation on the mechanism of the lineup of local dipoles in metallic $LiOsO_3$ is self-consistent.

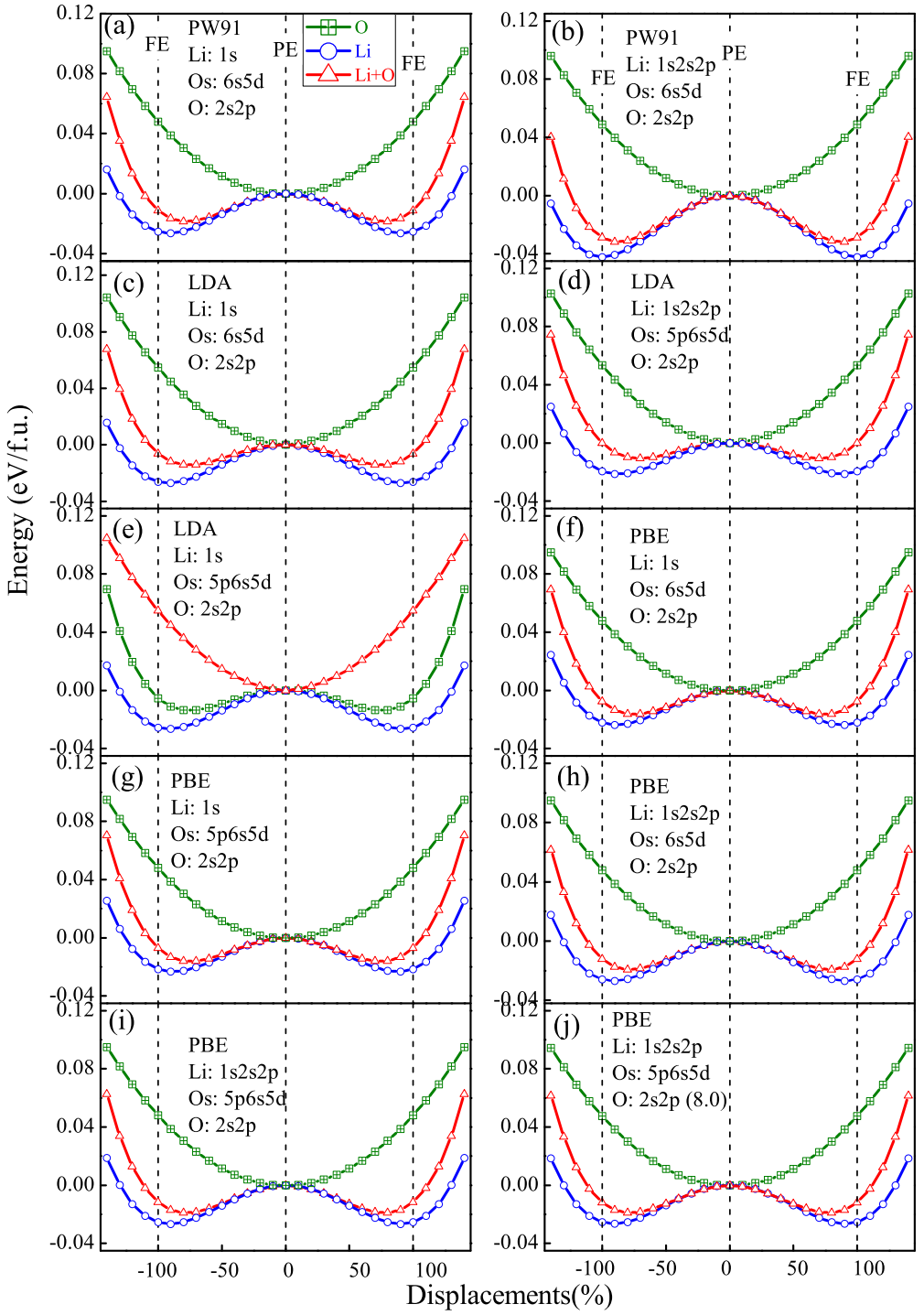

FIG. 6. (Color online) Potential-energy surface based on experimental displacements [6] using other available exchange-correlation functionals: (a, b) PW91. (c–e) LDA. (f–j) PBE. For each exchange-correlation functional, the calculations are performed using pseudopotentials with different valence electrons, and the used valence states for Li, Os, and O are inserted in related figures. The olive, blue, and red curves represent the potential-energy changes with respect to O displacements only, Li displacements only, and the coupled displacements of the Li and O ions. The total energy and displacements of PE states are set as zero. The displacements of corresponded FE states are set as 100%.

IV. SUMMARY

In summary, by performing DFT calculation, we investigate the microscopic mechanism of ferroelectricity in metallic $LiOsO_3$. We find that, in contrast to other 5*d* transition-metal oxides, for $LiOsO_3$, the effect of SOC is small and the electronic correlation is weak. We propose that the structural phase transition is of order-disorder type, and we find that the electronic states at the Fermi level are only weakly coupled to the ferroelectric-like transition, which makes the metallic ferroelectricity become possible, as discussed by Ref. [3]. In addition to that [3], by using a straightforward method,

TABLE II. The distances d_i (i = 1–6) and coupling parameters J_i (i = 1–6) between ith Li ion pairs.

NN	First	Second	Third	Fourth	Fifth	Sixth
d_i (Å)	3.66	5.06	5.28	6.25	6.61	7.32
J_i (meV)	− 4.2	− 0.16	− 1.9	− 0.17	− 0.06	− 0.27

we study the electric screening effect in this system and reveal that the screening in this compound, different from our previous thought for a metallic system, is strongly anisotropic. Therefore local dipole interactions along certain directions are not fully screened and result in the dipole ordering below a rather high temperature. We also want to emphasize that the above picture implied that the ferroelectric-like transition should be of order-disorder instead of displacive type. This is because the displacive-type ferroelectric transition occurring in ABO_3 perovskite structures is generally triggered by the hybridization between the B and O electronic states or the lone pair in the A site. In either case the change of the electric dipole will modify the valence band considerably. Therefore in a displacive system the dipole-dipole interaction will be strongly screened out in the metallic phase.

ACKNOWLEDGMENTS

H.M.L. is thankful to Z. Z. Du and Y. L. Wang for helpful discussions. The work was supported by National Key Project for Basic Research of China (Grants No. 2011CB922101, No. 2013CB922301, and No. 2014CB921104), NSFC (Grants No. 91122035, No. 51431006, No. 11374137, No. 61125403, and No. 11174124), and Doctoral Fund of Ministry of Education of China (Grant No. 20130091110003). The project is also funded by Priority Academic Program Development of Jiangsu Higher Education Institutions.

APPENDIX

We also calculate the potential-energy surface based on experimental displacements [6] by using available exchange-correlation functionals (such as local-density approximation, Perdew-Becke-Erzenhof, and PW91), and the results are presented in Fig. 6. In each case, a dense k mesh and huge energy cutoff for the basis set are carefully checked for better convergence. Adopting experimental coordinates will obtain unreasonable results, as the well depth caused by the sole Li ion movements is even larger than that of both the Li and O moments.

[1] W. Cochran, Adv. Phys. **9**, 387 (1960).
[2] P. W. Anderson and E. I. Blount, Phys. Rev. Lett. **14**, 217 (1965).
[3] D. Puggioni and J. M. Rondinelli, Nature Commun. **5**, 3432 (2014).
[4] I. A. Sergienko, V. Keppens, M. McGuire, R. Jin, J. He, S. H. Curnoe, B. C. Sales, P. Blaha, D. J. Singh, K. Schwarz, and D. Mandrus, Phys. Rev. Lett. **92**, 065501 (2004).
[5] V. Keppens, Nature Mater. **12**, 952 (2013).
[6] Y. Shi, Y. Guo, X. Wang, A. J. Princep, D. Khalyavin, P. Manuel, Y. Michiue, A. Sato, K. Tsuda, S. Yu, M. Arai, Y. Shirako, M. Akaogi, N. Wang, K. Yamaura, and A. T. Boothroyd, Nature Mat. **12**, 1024 (2013).
[7] H. Sim and B. G. Kim, Phys. Rev. B **89**, 201107(R) (2014).
[8] H. J. Xiang, Phys. Rev. B **90**, 094108 (2014).
[9] G. Giovannetti and M. Capone, Phys. Rev. B **90**, 195113 (2014).
[10] B. J. Kim, H. Jin, S. J. Moon, J.-Y. Kim, B.-G. Park, C. S. Leem, J. Yu, T. W. Noh, C. Kim, S.-J. Oh, J.-H. Park, V. Durairaj, G. Cao, and E. Rotenberg, Phys. Rev. Lett. **101**, 076402 (2008); H. Watanabe, T. Shirakawa, and S. Yunoki, *ibid.* **105**, 216410 (2010).
[11] X. Wan, A. M. Turner, A. Vishwanath, and S. Y. Savrasov, Phys. Rev. B **83**, 205101 (2011); B. J. Yang and Y. B. Kim, *ibid.* **82**, 085111 (2010).
[12] X. Wan, A. Vishwanath, and S. Y. Savrasov, Phys. Rev. Lett. **108**, 146601 (2012).
[13] Y. Du, X. Wan, L. Sheng, J. Dong, and S. Y. Savrasov, Phys. Rev. B **85**, 174424 (2012).
[14] R. Arita, J. Kuneš, A. V. Kozhevnikov, A. G. Eguiluz, and M. Imada, Phys. Rev. Lett. **108**, 086403 (2012).
[15] Y. G. Shi, Y. F. Guo, S. Yu, M. Arai, A. A. Belik, A. Sato, K. Yamaura, E. Takayama-Muromachi, H. F. Tian, H. X. Yang, J. Q. Li, T. Varga, J. F. Mitchell, and S. Okamoto, Phys. Rev. B **80**, 161104(R) (2009).
[16] S. Calder, V. O. Garlea, D. F. McMorrow, M. D. Lumsden, M. B. Stone, J. C. Lang, J.-W. Kim, J. A. Schlueter, Y. G. Shi, K. Yamaura, Y. S. Sun, Y. Tsujimoto, and A. D. Christianson, Phys. Rev. Lett. **108**, 257209 (2012).
[17] D. Khomskii, Physics **2**, 20 (2009).
[18] C.-G. Duan, J. P. Velev, R. F. Sabirianov, Z. Zhu, J. Chu, S. S. Jaswal, and E. Y. Tsymbal, Phys. Rev. Lett. **101**, 137201 (2008).
[19] G. Kresse and J. Hafner, Phys. Rev. B **47**, 558(R) (1993).
[20] G. Kresse, and J. Furthmüller, Phys. Rev. B **54**, 11169 (1996).
[21] J. P. Perdew, K. Burke, and M. Ernzerhof, Phys. Rev. Lett. **77**, 3865 (1996).
[22] R. E. Cohen, Nature (London) **358**, 136 (1992).
[23] N. A. Hill, J. Phys. Chem. B **104**, 6694 (2000).
[24] P. Ghosez, J.-P. Michenaud, and X. Gonze, Phys. Rev. B **58**, 6224 (1998).
[25] L. F. Mattheiss, Phys. Rev. B **13**, 2433 (1976).
[26] I. Inbar and R. E. Cohen, Phys. Rev. B **53**, 1193 (1996).